Effects of quantum well growth temperature on the recombination efficiency of InGaN/GaN multiple quantum wells that emit in the green and blue spectral regions

S. Hammersley, M. J. Kappers, F. C.-P. Massabuau, S.-L. Sahonta, P. Dawson, R. A. Oliver, and C. J. Humphreys

Citation: Applied Physics Letters **107**, 132106 (2015); doi: 10.1063/1.4932200

View online: http://dx.doi.org/10.1063/1.4932200

View Table of Contents: http://scitation.aip.org/content/aip/journal/apl/107/13?ver=pdfcov

Published by the AIP Publishing

Effects of quantum well growth temperature on the recombination efficiency of InGaN/GaN multiple quantum wells that emit in the green and blue spectral regions

S. Hammersley,[1] M. J. Kappers,[2] F. C.-P. Massabuau,[2] S.-L. Sahonta,[2] P. Dawson,[1] R. A. Oliver,[2] and C. J. Humphreys[2]
[1]*School of Physics and Astronomy, Photon Science Institute, University of Manchester, Manchester M13 9PL, United Kingdom*
[2]*Department of Materials Science and Metallurgy, University of Cambridge, 27 Charles Babbage Road, Cambridge CB3 0FS, United Kingdom*

(Received 31 July 2015; accepted 22 September 2015; published online 1 October 2015)

InGaN-based light emitting diodes and multiple quantum wells designed to emit in the green spectral region exhibit, in general, lower internal quantum efficiencies than their blue-emitting counter parts, a phenomenon referred to as the "green gap." One of the main differences between green-emitting and blue-emitting samples is that the quantum well growth temperature is lower for structures designed to emit at longer wavelengths, in order to reduce the effects of In desorption. In this paper, we report on the impact of the quantum well growth temperature on the optical properties of InGaN/GaN multiple quantum wells designed to emit at 460 nm and 530 nm. It was found that for both sets of samples increasing the temperature at which the InGaN quantum well was grown, while maintaining the same indium composition, led to an increase in the internal quantum efficiency measured at 300 K. These increases in internal quantum efficiency are shown to be due reductions in the non-radiative recombination rate which we attribute to reductions in point defect incorporation.
[http://dx.doi.org/10.1063/1.4932200]

Light emitting diodes (LEDs) based on InGaN/GaN quantum well (QW) active regions are now widely used when light in the blue and green regions of the visible spectrum is required. Despite their widespread use, some fundamental issues remain unsolved, for instance the external quantum efficiency (EQE) of devices designed to emit in the green[1] is, in general, considerably lower than that for blue emitters, e.g., EQEs 73% for blue emitters[2] have been reported. The lower efficiency as the emission wavelength increased is commonly referred to as the "green gap," as at green wavelengths, 540–590 nm, it is also not possible to produce efficient AlInGaP LEDs with an EQEs greater than 10%.[3,4]

The cause of the "green gap" is still a matter of debate, with the effects of large polarization fields in c-plane GaN based heterostructures often being held responsible. The In fraction in InGaN/GaN QWs required to achieve emission in the green part of the spectrum[5–7] is much higher than that required to achieve blue emission. The greater In fraction results in a much larger piezoelectric polarization, which causes the electron and hole wavefunction overlap to be reduced leading to longer radiative recombination times. If the non-radiative recombination pathways are similar then it can be anticipated that the efficiency of green light emission would be less than that of blue emission. However, it has been reported[8,9] that this change in the radiative recombination lifetime is not sufficient to fully explain the reduction in efficiency. It has been suggested that there is also a reduction in the non-radiative recombination lifetime. It is widely accepted that the high In fraction in InGaN QWs necessary to achieve green emission means that a relatively low growth temperature has to be used to negate the effects of In desorption during growth. It has been suggested that defect formation may occur as a consequence of either the higher In content or lower QW growth temperature, which may act as a contributory factor to the "green gap."[10] In particular, it has been shown that the use of low growth temperatures can lead to an increased density of structural defects[11] and impurity incorporation in GaN[12] and InGaN.[13] There is also a growing body of evidence that point defects are introduced into InGaN layers as the indium composition is increased.[14–17] For example, recent theoretical calculations have shown that nitrogen vacancies have the lowest formation energy in InN[18] or InGaN alloys with high indium compositions.[19] It has also been demonstrated that point defects act as non-radiative recombination centers, leading to a reduction in the non-radiative recombination lifetime.[20–22] In this paper, we will report on how the photoluminescence (PL) internal quantum efficiency (IQE) of sets of QW structures designed to emit at the same wavelength in the green and blue parts of the spectrum are influenced by the QW growth temperature.

All the multiple QW (MQW) samples were grown in a 6×2 in. Thomas Swan close-coupled showerhead reactor on GaN pseudo-substrates which consisted of about 4 μm of GaN on (0001) sapphire substrates.[23] The dislocation density for all the pseudo-substrates is ca. $4 \times 10^8\,\mathrm{cm}^{-2}$. The nominal thicknesses of the InGaN QWs and GaN barriers were 3 and 7 nm, respectively. InGaN growth was carried out using trimethylindium (TMI), trimethylgallium (TMG), and

ammonia (NH_3) as precursors and nitrogen as the carrier gas at a reactor pressure of 300 Torr. Throughout the QW and barrier growth, the ammonia flow was constant at 10 slm. Three blue 10-period QW samples (blue 1–3) and three green 5-period QW samples (green 1–3) were grown. For each set of samples, three different QW growth temperatures were chosen, as indicated in Table I (citing emissivity corrected surface temperatures). In order to ensure that the three blue and the three green MQW samples grown at the different temperatures had a constant peak emission wavelength, the TMI flux for the InGaN growth was varied (see Table I), while the TMG flux remained constant at 4.4 μmol/min, to compensate for the changes in indium incorporation rate. The GaN barriers were grown at a more optimal (higher) temperature using a two-temperature growth method,[23] which leads to gross well-width fluctuations (GWWFs). To characterize the thickness and composition of the QW stacks, X-ray diffraction (XRD) was employed, by performing an ω-2θ scan along the symmetric (002) reflection. Due to the presence of GWWFs, XRD could only tell us about the period, and average In composition of the structures, i.e., the combined thickness of the QWs and the barriers and the average composition of In. The results are summarized in Table I and confirm that the samples within each set have similar characteristics. For the optical measurements the samples were mounted to the cold finger of a temperature controlled (10–300 K) helium cryostat. Temperature and power dependent PL spectra were recorded under continuous wave excitation using a He/Cd laser with a photon energy of 3.815 eV. For PL decay measurements, the frequency tripled output of a mode-locked Ti:Sapphire laser, with a final photon energy of 4.881 eV was used to excite the samples. The PL time decay transients were processed using time correlated single photon counting techniques. All the optical measurements were performed using a Brewsters angle collection geometry in order to minimise the effects of Fabry-Pérot interference fringes.[24]

In Fig. 1, the low temperature (10 K) PL spectra recorded for all samples are shown. The sample sets designed to emit in the green (2.4 eV) or blue (2.7 eV) parts of the spectrum have very similar PL spectra with no significant or systematic differences in PL peak energy, line width, or line shape. The 300 K PL IQE was calculated by employing the widely[11,25–27] used methodology whereby it is assumed that the recombination in the sample at low temperature (10 K) is solely radiative[25,28,29] and thus the ratio of the integrated PL intensity at 300 K and 10 K is the IQE. The

TABLE I. Summary of the QW growth conditions and XRD results for the samples discussed in this paper.

Sample	QW growth T (°C)	TMI flow (μmol/min)	Period (nm)	In content (%)
Blue 1	748	9.7	9.7 ± 0.2	3.2 ± 0.5
Blue 2	730	2.0	9.8 ± 0.2	3.1 ± 0.5
Blue 3	716	1.3	9.7 ± 0.2	3.2 ± 0.5
Green 1	716	9.7	9.9 ± 0.2	5.1 ± 0.5
Green 2	706	4.8	9.9 ± 0.2	5.2 ± 0.5
Green 3	698	3.5	10.0 ± 0.2	5.1 ± 0.5

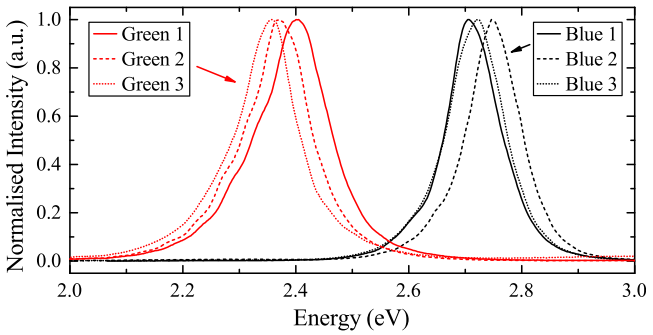

FIG. 1. 10 K PL spectra for the green-emitting QW structures and blue-emitting QW structures.

variation of IQE with excitation power density at 300 K is shown in Fig. 2 for all samples.

First, we turn our attention to the IQE values at the lowest excitation power used, i.e., 4 W cm^{-2}. In general, the IQE of the blue samples is greater than the green set with the IQE values for both sets increasing with increases in growth temperature. This overall behavior is in line with the suggestion that increasing the growth temperature leads to a reduction in the incorporation of defect centers that can provide non-radiative recombination paths. Before such a conclusion can be confirmed, it is vital to know whether the radiative lifetime has also been influenced by changes in the growth temperature. This is particularly important in the case of InGaN QWs as the radiative lifetime is not only governed by the electron/hole wavefunction separation perpendicular to the growth plane but also the local microstructure that can influence the in-plane wavefunction overlap.[30] By recording the PL decay transients at 10 K, as shown in Fig. 3, we obtain a measure of the radiative recombination lifetime at the luminescence peak. Based on the assumption that every excitation photon produces an electron/hole pair and these are equally distributed amongst the QWs, the peak carrier densities per QW were calculated to be $\sim 4 \times 10^{11}$ cm^{-2} pulse^{-1} QW^{-1} for the blue-emitting samples and $\sim 8 \times 10^{11}$ cm^{-2} pulse^{-1} QW^{-1} for the green-emitting samples. The difference between maximum peak carrier densities is due to the blue and green emitting samples containing 10 and 5 QWs, respectively. However, it should be noted that the forms of the PL decay curves are independent of the initial peak carrier density. As shown in Fig. 3(a), the samples that emit in the green had essentially identical PL decay curves. If we define the PL lifetime as the time taken for the PL intensity to fall from its maximum to 1/e of that value, the decay times for the green emitting samples lay in the range of 130–160 ± 15 ns with no systematic variation with changes in the QW growth temperature. For the blue emitting samples, sample blue 1 had a PL decay time of 22 ± 2 ns, and samples blue 2 and blue 3 had a PL decay times of 15 ± 2 ns. The reason for the difference in PL decay lifetime for sample blue 1 compared to samples blue 2 and 3 is not clear but it is not regarded as significant in the context of this investigation. This is because, if anything, the slower radiative recombination rate of blue 1 would lead to a reduction in the IQE at 300 K, which is not in line with our observations. Thus, we conclude from the lack of any significant differences in PL decay lifetimes at

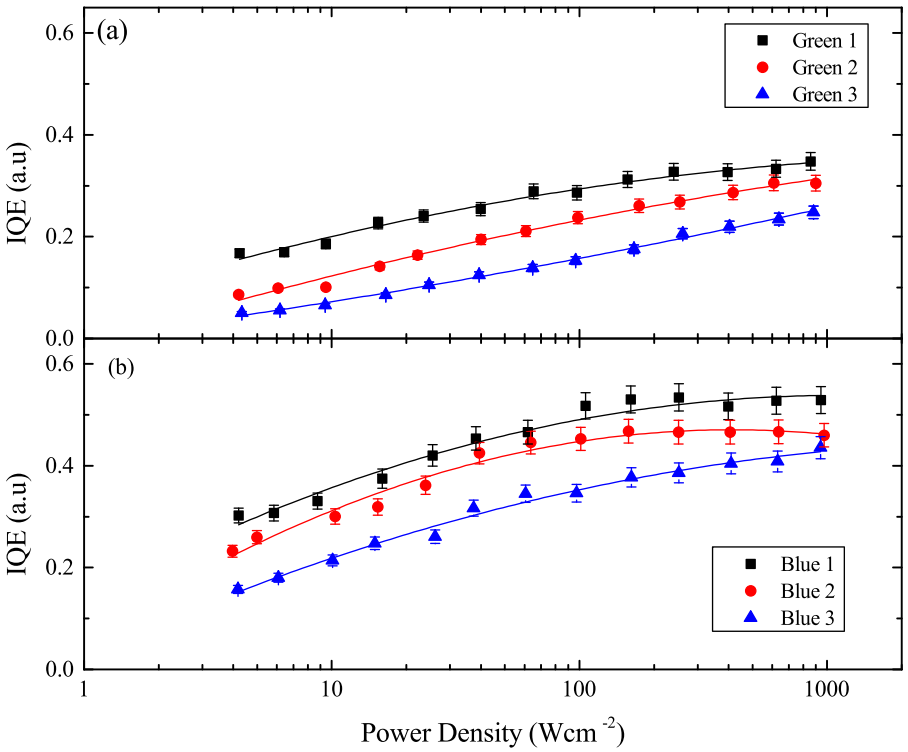

FIG. 2. 300 K IQE as a function of excitation power density for (a) the green-emitting and (b) the blue-emitting structures.

10 K within the blue and green emitting sample sets that adjusting the growth temperature in each of the sample sets has not had any significant effect on the factors that govern the radiative recombination lifetimes. We can therefore assume that any changes in the radiative recombination lifetimes with temperature will affect each sample equally and therefore any changes amongst the samples that develop are a result of changes in the non-radiative lifetime.

Returning to the 300 K IQE data, we also measured PL decay transients at 300 K at the peak of the spectra, as shown in Fig. 4. Unlike the results obtained at 10 K, there are now systematic variations in the PL decay curves as a function of QW growth temperature within both sets of samples, with the most marked differences being observed for the green-emitting samples. This variation in lifetime is compatible with the changes in IQE being caused by differences in non-radiative recombination, with the non-radiative recombination lifetime decreasing as the QW growth temperature is reduced. To ensure that these results are not complicated by droop related processes, the measurements were carried out at excitation carrier densities below the onset of efficiency droop.[31]

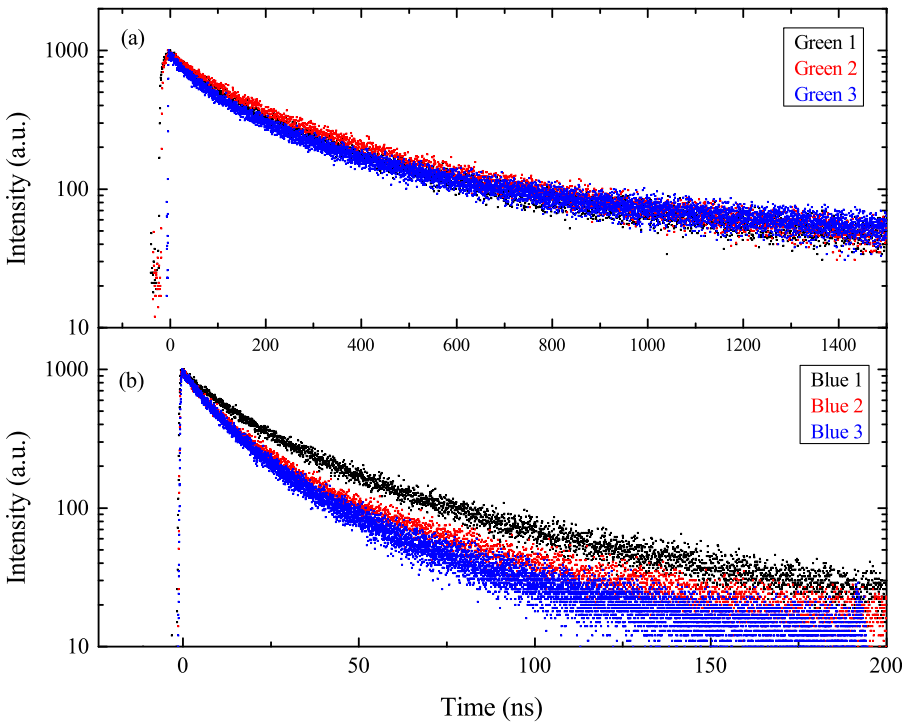

FIG. 3. 10 K PL decay transients detected at the PL emission peak for (a) the green-emitting and (b) the blue emitting samples.

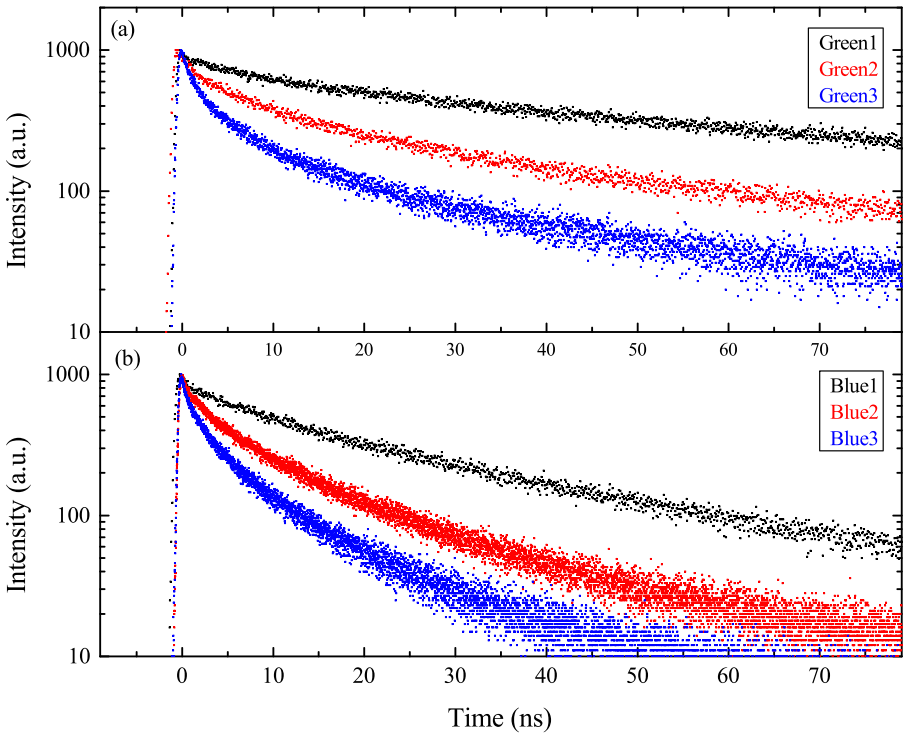

FIG. 4. 300 K PL decay transients detected at the PL emission peak for (a) the green-emitting and (b) the blue emitting samples.

All of the samples in both sets exhibited the same overall behavior, with the IQE rising as the excitation power density was increased (see Fig. 2). As the excitation power density is increased, the IQE values increase in a similar manner until at the highest excitation power densities, where the rate of increase slows until a plateau is reached, a behavior observed prior to the onset of efficiency droop.[32] Such progressive increases in IQE or PL intensity with increasing excitation density have been widely reported[32–37] and have been attributed to saturation of a non-radiative recombination pathway.[37] Above the excitation power density at which the IQE begins to reach a plateau, the behavior of samples blue 1 and blue 2 begins to diverge with the IQE of blue 2 reaching a stable IQE at a lower excitation power density than blue 1. The reason for this is not, as yet, clear but presumably is related to the precise nature of the process responsible for droop.[32–37] Clearly the behavior of blue 3 is very different from the other samples in this set. For the sample blue 3, at the lowest excitation power density the IQE value is much lower than blue 1 and blue 2 presumably reflecting the increase in the density of defects incorporated at the lower QW growth temperature. Again as the excitation power density increases the IQE for blue 3 also increases, but although the rate of increase of IQE with increasing excitation power density reduces, droop is not observed for this sample. We suggest that this is because of enhanced non-radiative recombination in this sample compared with the other two prevents the equilibrium carrier density reaching the critical value for the onset of droop.

Next, we turn our attention to the behavior of the samples that emit at a longer wavelength, i.e., green 1, green 2, and green 3. First, we note that the IQE of blue 3 is greater than green 1. Since these samples were grown at the same temperature and assuming similar levels of defect incorporation, the lower IQE for green 1 reflects the longer radiative lifetime of carriers in this sample. At the lowest excitation power density, the IQE values of all the green samples increase systematically with increasing growth temperature (see Fig. 2(a)). We interpret this behavior as reflecting the increased incorporation of non-radiative defects with decreasing growth temperature. Although the IQE of all three samples increases with increasing excitation power density, the trend in IQE as a function of growth temperature remains for all excitation power densities investigated. At the highest excitation power density, there is no evidence of efficiency droop, presumably reflecting the fact that the carrier density is not sufficiently high to trigger the process responsible for droop. The particular aspect of this data that is most relevant to the question of the green gap is that the effect of higher QW growth temperature is maintained at the highest excitation power density which we estimate is equivalent to the operating currents of LEDs.

In summary, we have investigated the optical properties of two sets of InGaN/GaN MQW samples grown at varying QW growth temperatures with one set emitting in the blue and one in the green spectral region. PL decay transients measured at 10 K showed that the change in QW growth temperature did not have a significant effect on the PL decay timescale. However, at 300 K a clear systematic variation in PL decay timescale was observed, with lower QW growth temperatures resulting in faster PL decay transients. The recombination decay curves at 300 K are a combination of radiative and non-radiative processes. As the timescale for radiative recombination is unaffected by growth temperature in both sample sets as revealed by the time decay curves measured at 10 K, we attribute the changes in PL decay curves observed at room temperature to a reduction in non-radiative recombination timescale as the QW growth temperature is reduced. We ascribe this change in the non-radiative recombination timescale to an increase in the density of defects incorporated at lower QW growth temperatures. This conclusion was supported by IQE measurements at 300 K

conducted as a function of excitation. For both sets of samples, the IQE increased with increasing QW growth temperature over the majority of the excitation power density range covered. This behavior was observed even at the highest level of excitation suggesting that the QW growth temperature could play a role in determining the relative performance of blue and green LEDs at high operating currents.

This work was carried out with the financial support of the United Kingdom Engineering and Physical Sciences Research Council under Grant Nos. EP/I012591/1 and EP/H011676/1. All data created during this research are openly available from the University of Manchester eScholar archive at http://dx.doi.org/10.15127/1.269741.

[1]H.-Y. Ryu, G.-H. Ryu, S.-H. Lee, and H.-J. Kim, J. Korean Phys. Soc. **63**, 180–184 (2013).
[2]M. J. Cich, R. I. Aldaz, A. Chakraborty, A. David, M. J. Grundmann, A. Tyagi, M. Zhang, F. M. Steranka, and M. R. Krames, Appl. Phys. Lett. **101**, 223509 (2012).
[3]M. Krames, O. Shchekin, R. Mueller-Mach, G. O. Mueller, L. Zhou, G. Harbers, and M. Craford, J. Disp. Technol. **3**, 160–175 (2007).
[4]A. Löffler and M. Binder, Compd. Semicond. **19**(7), 32–36 (2013).
[5]Z. Lin, R. Hao, G. Li, and S. Zhang, Jpn. J. Appl. Phys., Part 1 **54**, 022102 (2015).
[6]K. P. O'Donnell, M. Auf der Maur, A. Di Carlo, K. Lorenz, and SORBET Consortium, Phys. Status Solidi RRL **6**, 49–52 (2012).
[7]S. Chichibu, T. Azuhata, T. Sota, and S. Nakamura, Appl. Phys. Lett. **69**, 4188–4190 (1996).
[8]T. Langer, A. Kruse, F. A. Ketzer, A. Schwiegel, L. Hoffmann, H. Jnen, H. Bremers, U. Rossow, and A. Hangleiter, Phys. Status Solidi C **8**, 2170–2172 (2011).
[9]T. Langer, H. Jnen, A. Kruse, H. Bremers, U. Rossow, and A. Hangleiter, Appl. Phys. Lett. **103**, 022108 (2013).
[10]M. H. Crawford, IEEE J. Sel. Top. Quantum Electron. **15**, 1028–1040 (2009).
[11]F.-P. Massabuau, M. Davies, F. Oehler, S. Pamenter, E. Thrush, M. Kappers, A. Kovács, T. Williams, M. Hopkins, C. Humphreys *et al.*, Appl. Phys. Lett. **105**, 112110 (2014).
[12]D. Koleske, A. Wickenden, R. Henry, and M. Twigg, J. Cryst. Growth **242**, 55–69 (2002).
[13]M. J. Kappers, T. Zhu, S.-L. Sahonta, C. J. Humphreys, and R. A. Oliver, Phys. Status Solidi C **12**, 403–407 (2015).
[14]A. Armstrong, M. Crawford, and D. Koleske, J. Electron. Mater. **40**, 369–376 (2011).
[15]E. Gr, Z. Zhang, S. Krishnamoorthy, S. Rajan, and S. A. Ringel, Appl. Phys. Lett. **99**, 092109 (2011).
[16]A. Armstrong, T. A. Henry, D. D. Koleske, M. H. Crawford, and S. R. Lee, Opt. Express **20**, A812–A821 (2012).
[17]A. Uedono, S. Ishibashi, N. Oshima, R. Suzuki, and M. Sumiya, ECS Trans. **61**, 19–30 (2014).
[18]A. Janotti, J. L. Lyons, and C. G. Van de Walle, Physica Status Solidi A **209**, 65–70 (2012).
[19]T. Obata, J. Ichi Iwata, K. Shiraishi, and A. Oshiyama, J. Cryst. Growth **311**, 2772–2775 (2009).
[20]T. Langer, H.-G. Pietscher, H. Bremers, U. Rossow, D. Menzel, and A. Hangleiter, Proc. SPIE **8625**, 862522 (2013).
[21]S. F. Chichibu, A. Uedono, T. Onuma, T. Sota, B. A. Haskell, S. P. DenBaars, J. S. Speck, and S. Nakamura, Appl. Phys. Lett. **86**, 021914 (2005).
[22]D. Look, D. Reynolds, Z.-Q. Fang, J. Hemsky, J. Sizelove, and R. Jones, Mater. Sci. Eng., B **66**, 30–32 (1999).
[23]R. A. Oliver, F. C.-P. Massabuau, M. J. Kappers, W. A. Phillips, E. J. Thrush, C. C. Tartan, W. E. Blenkhorn, T. J. Badcock, P. Dawson, M. A. Hopkins, D. W. E. Allsopp, and C. J. Humphreys, Appl. Phys. Lett. **103**, 141114 (2013).
[24]D. M. Graham, A. Soltani-Vala, P. Dawson, M. J. Godfrey, T. M. Smeeton, J. S. Barnard, M. J. Kappers, C. J. Humphreys, and E. J. Thrush, J. Appl. Phys. **97**, 103508 (2005).
[25]A. Hangleiter, D. Fuhrmann, M. Grewe, F. Hitzel, G. Klewer, S. Lahmann, C. Netzel, N. Riedel, and U. Rossow, Phys. Status Solidi A **201**, 2808–2813 (2004).
[26]M. J. Davies, P. Dawson, F. C.-P. Massabuau, F. Oehler, R. A. Oliver, M. J. Kappers, T. J. Badcock, and C. J. Humphreys, Phys. Status Solidi C **11**, 750–753 (2014).
[27]M. J. Davies, F. C.-P. Massabuau, P. Dawson, R. A. Oliver, M. J. Kappers, and C. J. Humphreys, Phys. Status Solidi C **11**, 710–713 (2014).
[28]C. E. Martinez, N. M. Stanton, A. J. Kent, D. M. Graham, P. Dawson, M. J. Kappers, and C. J. Humphreys, J. Appl. Phys. **98**, 053509 (2005).
[29]D. Fuhrmann, C. Netzel, U. Rossow, A. Hangleiter, G. Ade, and P. Hinze, Appl. Phys. Lett. **88**, 071105 (2006).
[30]A. Morel, P. Lefebvre, S. Kalliakos, T. Taliercio, T. Bretagnon, and B. Gil, Phys. Rev. B **68**, 045331 (2003).
[31]M. J. Davies, T. J. Badcock, P. Dawson, M. J. Kappers, R. A. Oliver, and C. J. Humphreys, Appl. Phys. Lett. **102**, 022106 (2013).
[32]S. Hammersley, D. Watson-Parris, P. Dawson, M. Godfrey, T. Badcock, M. Kappers, C. McAleese, R. Oliver, and C. Humphreys, J. Appl. Phys. **111**, 083512 (2012).
[33]Y. C. Shen, G. O. Mueller, S. Watanabe, N. F. Gardner, A. Munkholm, and M. R. Krames, Appl. Phys. Lett. **91**, 141101 (2007).
[34]M.-H. Kim, M. F. Schubert, Q. Dai, J. K. Kim, E. F. Schubert, J. Piprek, and Y. Park, Appl. Phys. Lett. **91**, 183507 (2007).
[35]I. Rozhansky and D. Zakheim, Semiconductors **40**, 839–845 (2006).
[36]M. F. Schubert, J. Xu, Q. Dai, F. W. Mont, J. K. Kim, and E. F. Schubert, Appl. Phys. Lett. **94**, 081114 (2009).
[37]H. Murotani, Y. Yamada, Y. Honda, and H. Amano, Phys. Status Solidi B **252**, 940–945 (2015).